

Formation Condition of Quantum Well States in Oxide Nanostructures

Some oxide nanostructures have recently been shown to host quantum well (QW) states that are promising for quantum device applications by designing the wave function of their strongly correlated electrons. However, it is unclear why QW states only appear in certain oxide nanostructures, limiting the possibilities of wave-function engineering. Here, we demonstrate that the electron mean free path λ is one of the essential conditions to form standing waves of strongly correlated electrons in oxide nanostructures. *In situ* angle-resolved photoemission spectroscopy experiments reveal that the intensity of the QW states is almost linearly correlated to λ and may disappear at the Ioffe–Regel criterion, corresponding to the nearest neighbor inter-vanadium distance in $\text{SrTi}_{1-x}\text{V}_x\text{O}_3$. Our findings provide design guidelines for creating and controlling novel quantum phenomena in oxide nanostructures.

Quantum confinement of strongly correlated electrons in oxide artificial structures has provided an opportunity to better understand the fundamental low-dimensional phenomena of strongly correlated electron systems and attracted considerable interest for its potential technological application in future oxide electronics [1]. Dimensionality reduction changes the complex interaction among the spin, charge, and orbital degrees of freedom of the correlated electrons, yielding unusual quantum phenomena. However, quantized states have not been observed in all conductive correlated oxides [2]. Thus, it is essential to determine the conditions that result in realizing the quantum-well (QW) states in strongly correlated oxides. Since the QW states are caused by the standing waves of electrons confined in space by a potential well, which are characterized by the quantum number n , that is, the number of half-wavelengths that span the well, the appearance of QW states may

closely be related to the mean free path λ of the electrons, as well as the reflectivity of the electrons at the potential walls (surface and interface). Assuming high reflectivity at the surface and interface, the formation of the standing waves (quantization states) may strongly depend on the relationship between λ and the width of QW structure (layer thickness) L .

In this study, we selected $\text{SrTi}_{1-x}\text{V}_x\text{O}_3$ (STVO) ultrathin films epitaxially grown on Nb-doped SrTiO_3 to investigate the relationship between λ and the appearance of quantization states. Our previous work has demonstrated that λ can be linearly controlled by varying x in STVO [3]. By adopting the STVO QW structures, we examined the relationship between λ and QW formation using *in situ* angle-resolved photoemission spectroscopy (ARPES). The controllability of λ in STVO enables us to examine the evolution of QW states with varying x .

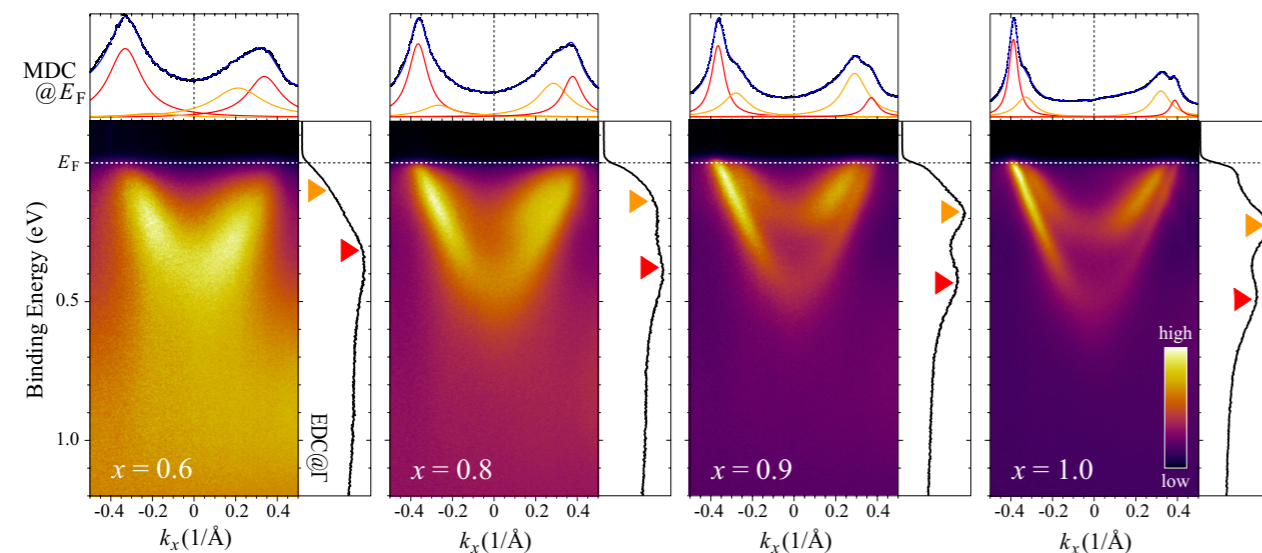


Figure 1: *In situ* ARPES intensity plot along the Γ – X direction for STVO QW structures of 6 monolayers with $x = 0.6$ – 1.0 . The MDCs at E_F are shown at the top of the respective ARPES images, while the EDCs at the Γ point are on the right-hand side of each image. The red and orange arrows in the EDCs indicate the $n = 1$ and $n = 2$ quantization energies (bottom energies of subbands), respectively. In the MDCs, the fitting results for $n = 1$, $n = 2$, and total are overlaid by red, orange, and blue curves, respectively.

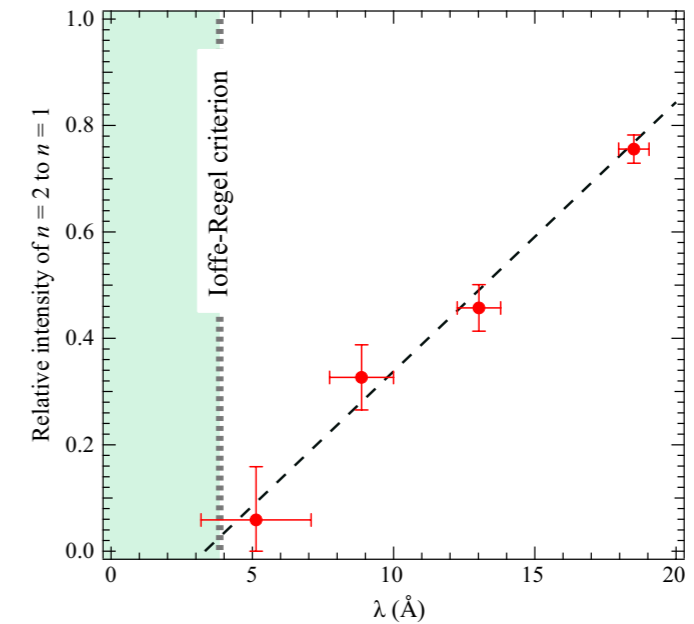


Figure 2: The relative intensity (area under the curve) of $n = 2$ to $n = 1$ states is plotted as a function of $\lambda_{n=1}$ (red-filled circles). The values of λ are estimated from the respective MDCs at E_F . The IR criterion ($\lambda_{\text{IR}}^{\text{min}} = a$) for STVO is indicated by a dotted line.

Figure 1 shows *in situ* ARPES intensity map along the Γ – X direction for STVO QW structures with $x = 0.6$ – 1.0 . In the case of SrVO_3 (STVO with $x = 1.0$) film, clear parabolic subband dispersions are observed. According to previous studies [4], the observed QW states correspond to subbands with quantum numbers $n = 1$ (red) and 2 (orange). As x decreases, the relative intensity of $n = 2$ to $n = 1$ states significantly weakens, and $n = 2$ states seem to almost disappear at $x = 0.6$, although the $n = 1$ states are still visible. Meanwhile, in the momentum distribution curve (MDC) at the Fermi level (E_F), the peak width significantly increases with reducing x . Since the MDC width corresponds to $1/\lambda$ [3], the broadening of the MDC peak indicates that the λ value decreases with decreasing x . The observed correlation between the QW states and λ demonstrates that λ plays one of the essential roles in forming quantization states in correlated conductive oxides.

In order to see the spectral behavior in further detail, we extract the QW states from the energy distribution curves (EDCs) at the Γ point and plot in **Fig. 2** the relative intensity (area under the curve) of $n = 2$ to $n = 1$ as a function of λ for $n = 1$ ($\lambda_{n=1}$) that is estimated from the MDCs at E_F . It can be observed from **Fig. 2** that the relative intensity of $n = 2$ to $n = 1$ is proportional to λ , clearly demonstrating a proportional relationship between the formation of QW states and λ . In **Fig. 2**, the Ioffe–Regel (IR) criterion ($\lambda_{\text{IR}}^{\text{min}}$) for STVO that corresponds to the interatomic spacing a of STVO ($\lambda_{\text{IR}}^{\text{min}} = 3.82 - 3.91 \text{ \AA}$) is overlaid. The line

fit for the data (dashed line) suggests that the QW states may vanish around the $\lambda_{\text{IR}}^{\text{min}}$, implying that the condition of QW-state formation is responsible for the IR criterion ($\lambda > a$). These results indicate that λ plays a decisive role in the formation of QW states. Our findings provide design guidelines for creating and controlling novel quantum phenomena in oxide nanostructures [5].

REFERENCES

- [1] R. Yukawa, M. Kobayashi, T. Kanda, D. Shiga, K. Yoshimatsu, S. Ishibashi, M. Minohara, M. Kitamura, K. Horiba, A. F. Santander-Syro and H. Kumigashira, *Nat. Commun.* **12**, 7070 (2021).
- [2] E. Cappelli, W. O. Tromp, S. M. K. Walker, A. Tamai, M. Gibert, F. Baumberger and F. Y. Bruno, *APL Mater.* **8**, 051102 (2020).
- [3] T. Kanda, D. Shiga, R. Yukawa, N. Hasegawa, D. K. Nguyen, X. Cheng, R. Tokunaga, M. Kitamura, K. Horiba, K. Yoshimatsu and H. Kumigashira, *Phys. Rev. B* **104**, 115121 (2021).
- [4] K. Yoshimatsu, T. Okabe, H. Kumigashira, S. Okamoto, S. Aizaki, A. Fujimori and M. Oshima, *Phys. Rev. Lett.* **104**, 147601 (2010).
- [5] T. Kanda, D. Shiga, A. Wada, R. Hayasaka, Y. Masutake, N. Hasegawa, M. Kitamura, K. Yoshimatsu and H. Kumigashira, *Commun. Mater.* **4**, 27 (2023).

BEAMLINE

BL-2A

T. Kanda¹, D. Shiga¹, A. Wada¹, R. Hayasaka¹, Y. Masutake¹, N. Hasegawa¹, M. Kitamura^{2,3}, K. Yoshimatsu¹ and H. Kumigashira¹ (¹Tohoku Univ., ²KEK-IMSS-PF, ³QST)